Protein kinase C and calcineurin cooperatively mediate cell survival under compressive mechanical stress

Ranjan Mishra[a,b], Frank van Drogen[a], Reinhard Dechant[a], Soojung Oh[c], Noo Li Jeon[c,d], Sung Sik Lee[a,e,1], and Matthias Peter[a,1]

[a]Institute of Biochemistry, Department of Biology, ETH Zürich, 8093 Zürich, Switzerland; [b]Molecular Life Science PhD Program, Life Science Zürich Graduate School, CH-8057 Zürich, Switzerland; [c]Department of Mechanical & Aerospace Engineering, Seoul National University, 08826 Seoul, Republic of Korea; [d]Institute of Advanced Machinery and Design, Seoul National University, 08826 Seoul, Republic of Korea; and [e]Scientific Center for Optical and Electron Microscopy, ETH Zürich, 8093 Zürich, Switzerland

Edited by David A. Weitz, Harvard University, Cambridge, MA, and approved November 6, 2017 (received for review May 31, 2017)

Cells experience compressive stress while growing in limited space or migrating through narrow constrictions. To survive such stress, cells reprogram their intracellular organization to acquire appropriate mechanical properties. However, the mechanosensors and downstream signaling networks mediating these changes remain largely unknown. Here, we have established a microfluidic platform to specifically trigger compressive stress, and to quantitatively monitor single-cell responses of budding yeast in situ. We found that yeast senses compressive stress via the cell surface protein Mid2 and the calcium channel proteins Mid1 and Cch1, which then activate the Pkc1/Mpk1 MAP kinase pathway and calcium signaling, respectively. Genetic analysis revealed that these pathways work in parallel to mediate cell survival. Mid2 contains a short intracellular tail and a serine–threonine-rich extracellular domain with spring-like properties, and both domains are required for mechanosignaling. Mid2-dependent spatial activation of the Pkc1/Mpk1 pathway depolarizes the actin cytoskeleton in budding or shmooing cells, thereby antagonizing polarized growth to protect cells under compressive stress conditions. Together, these results identify a conserved signaling network responding to compressive mechanical stress, which, in higher eukaryotes, may ensure cell survival in confined environments.

mechanosensor | Pkc1/Mpk1 pathway | calcium signaling | cell polarity | microfluidics

In the physiological environment, cells are constantly exposed to a variety of mechanical cues such as shear stress, tensile stress, and compressive stress. For instance, leukocytes and disseminating cancer cells experience shear stress in blood circulation (1–4) and experience compressive stress when they migrate through capillary and confined tissue microenvironments (1, 5). Similarly, cells in solid tumors experience growth-induced compression (6), which triggers an invasive phenotype (7). Thus, the cellular response to such stimuli in a microenvironment underlies physiological processes relevant for health and disease.

To respond to physical cues, cells modulate their intracellular organization and alter their microenvironment. While the mechanisms regulating cellular responses to compression stress remain largely unknown, integrin-dependent reorganization of the actin cytoskeleton adjusts mechanical properties in response to shear and stretching/tensile stress (7–11). Likewise, cell confinement in narrow constrictions redirects the actin cytoskeleton and allows amoeboid-type cell motility (8), in part by organizing perinuclear actin to protect the nucleus (12). Mechanostress triggered by urine flow in the kidney results in calcium influx through stretch-activated calcium channels (13, 14). Similarly, yeast cells are thought to translate mechanical stimuli into an increase in intracellular calcium concentration via a calcium channel composed of a heteromeric assembly of Mid1 and Cch1. Recent evidence also implicates the target of rapamycin complex 2 (TORC2) pathway in mechanotransduction (15). Indeed, membrane tension induced by mechanically stretching the plasma membrane redistributes Slm proteins from eisosomes to activate TORC2, which, in turn, regulates actin polarization and endocytosis to modulate membrane composition.

However, the lack of suitable experimental systems to trigger a specific mechanostress response impedes discovery of physiological responses and dissection of the mechanism of force sensing and the downstream signaling networks. To overcome this limitation, we developed a microfluidic device coupled with quantitative live-cell imaging, which allows monitoring the response of single cells to compressive stress. Interestingly, we found that, through the sensors Mid1 and Mid2, mechanical stress specifically activates calcium signaling and the cell wall integrity (CWI) pathway, respectively, and these pathways cooperate to prevent cell lysis, at least in part by inhibiting polarized growth both during budding and mating. As these signaling pathways are conserved in mammals, we speculate that similar mechanisms orchestrate the response of cells exposed to mechanical stress in complex microenvironments.

Results

A Microfluidic Platform for Studying Mechanotransduction in Budding Yeast. To study cellular responses of budding yeast to compressive mechanical stress, we developed a microfluidic device coupled with quantitative live-cell imaging, which allows monitoring the response of single yeast cells to compressive stress (Fig. 1 *A* and *B* and Fig. S1). The device is composed of a multilayer chip

Significance

Cells are constantly exposed to a variety of mechanical cues, and respond by activating conserved signaling pathways that modulate their profiliation and intracellular organization. For instance, cells in solid tumors experience sustained compression from the microenvironment, and compressive stress is known to trigger an invasive phenotype in some cancer cells. However, despite its importance for health and disease, the specific mechanosensors and the downstream signaling network mediating these physiological responses remain largely unknown, in part due to the lack of appropriate experimental systems. Here, we develop a microfluidic platform that allows triggering compressive mechanical stress in a reversible and controllable manner, and we identify cell surface receptors that specifically sense compressive mechanical stress and generate synergistic cellular responses.

Author contributions: R.M., F.v.D., R.D., S.S.L., and M.P. designed research; R.M. and S.S.L. performed research; R.M., S.O., N.L.J., and S.S.L. contributed new reagents/analytic tools; R.M. and S.S.L. analyzed data; and R.M., S.S.L., and M.P. wrote the paper.

The authors declare no conflict of interest.

This article is a PNAS Direct Submission.

[1]To whom correspondence may be addressed. Email: sungsik.lee@scopem.ethz.ch or matthias.peter@bc.biol.ethz.ch.

This article contains supporting information online at www.pnas.org/lookup/suppl/doi:10.1073/pnas.1709079114/-/DCSupplemental.

with two polydimethylsiloxane (PDMS) layers bonded to a glass coverslip at the bottom. The upper PDMS layer has four air channels that are aligned onto eight cell chambers imprinted in the lower PDMS membrane. Each cell chamber has a micropatch of pillars hanging toward the coverslip (Fig. 1*A* and Fig. S1). Cells are loaded into the cell chambers by flowing them along the microchannels connecting the cell chambers, using pressure from the digital controller. Application of pressure in the air channel pushes the micropillars from the lower PDMS membrane down, causing the micropillars to make contact with the cells underneath. As PDMS is a deformable soft polymer, the increased pressure in the air channels results in mechanical forces applied to trapped cells. The applied force leads to cellular deformation and a corresponding perimeter change as the cell expands in the x and y axes, yielding an increased apparent cell area when cells are viewed from above, which we call "top view." Thus, the increase in cell top view area was measured, providing an indirect measurement of the mechanical pressure experienced by the cells (Fig. 1 *B* and *C*).

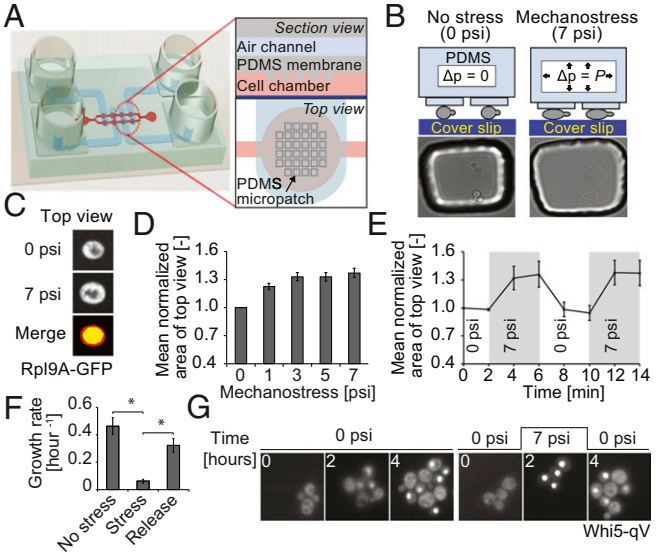

Fig. 1. A microfluidic device to study mechanotransduction in budding yeast. (*A*) Schematic representation of the microfluidic device used to trigger mechanostress. The microfluidic chip is made of two layers of soft elastic polymer, PDMS, bonded to glass coverslip on the bottom. See *Results* and *Supporting Information* for details. (*B*) Mechanostress is applied to budding yeast cells trapped in the microfluidic chip coated with concanavalin A. By applying pressure in the air channels, the PDMS micropillars are pushed toward the coverslip, thereby compressing cells trapped below the pillars as illustrated in the schematic drawing. Cells before and after application of mechanostress are shown in microscopy images. (*C*) Cell perimeter changes as the cell expands in the x and y axes, changing the apparent cell area when cells are viewed from above (top view). Cells expressing Rpl9A-GFP as a cytoplasmic marker were imaged before (0 psi) and after application of 7 psi pressure. Representative images show the top view as maximum intensity projections. The change in cell top view area with mechanostress was measured. Images before (yellow) and after (red) mechnostress were merged to visualize the increase in cell top view area upon mechamostress. (*D*) The area of cells expressing Rpl9A-GFP was quantified using maximum intensity projections, normalized to the original area, and plotted as a function of pressure applied in the air channel from the digital controller. The error bars indicate the SEM for at least 50 cells analyzed for each condition. (*E*) The reversibility of the microfluidic device was tested by applying 7 psi at the indicated times, and was quantified every 2 min as the mean area of top view normalized to the original area. See also Movie S1. For each time point, at least 50 cells were analyzed. The SEM is depicted as error bars. (*F*) The change in cell number was quantified for cells growing for 3 h without stress, after applying mechanostress (7 psi), and 3 h after pressure release. As cells would have overpopulated the cell chamber with 9 h of continuous growth, experiments were performed in two sets. In one set, cells were grown in the chip for 3 h without pressure, and then pressure was applied for another 3 h. In the second set, pressure was applied for first 3 h and then released for another 3 h. The error bars indicate the SE of mean of three experiments. A Student's t test was performed, and the significances were compared with the mechanostressed condition indicated (*$P < 0.05$). (*G*) Mechanostress (7 psi) was applied for 2 h to cells expressing Whi5-qV, and the localization of Whi5-qV was analyzed by fluorescence microscopy at the times indicated. See also Movies S2 and S3. Note that cells exposed to mechanostress arrest with nuclear accumulation of Whi5-qV. Images are taken with objective lens (magnification: *B* and *G*, 60×; *C*, 100×).

To deduce the optimal pressure to activate the cellular mechanostress response, we measured the top view area when cells were exposed to increasing pressure. To facilitate segmentation and improve the area measurements, we used maximum intensity projected fluorescent images of cells expressing GFP-labeled Rpl9A (Rpl9A-GFP), a highly abundant cytoplasmic protein. The mean values were then normalized and plotted against the applied pressure. As shown in Fig. 1*D*, the top view area increased gradually to a maximum of 30%, saturating when ~3 psi was applied from the digital controller. To ensure that all cells are maximally compressed, we used 7 psi in most of our experiments. This pressure level is also physiologically relevant, as yeast cells can experience up to about 100 psi (0.7 MPa) when grown in confined geometries, which leads to stalled growth (16, 17). Importantly, cells rapidly return to their original size after pressure release, and subsequent reapplication of pressure restored the top view area to the maximum of about 30% increase (Fig. 1*E* and Movie S1). Thus, mechanostress applied by this microfluidic device is reversible, and our results indicate that cells are elastic and regain their original shape in z axis after pressure release. Moreover, cell deformation rates in z axis allowed estimating the stiffness of living yeast cells to a Young's modulus of G = 0.09 MPa to 0.57 MPa (*SI Text*).

To investigate the physiological response to mechanostress, we compared the growth rate of nonstressed cells with that of cells exposed to compressive stress for 3 h. In contrast to unstressed cells, the growth rate increased only marginally upon compressive stress (Fig. 1*F*). However, after pressure release, the arrested cells efficiently restarted proliferation with a growth rate comparable to that of nonstressed cells. To further characterize this cell cycle defect, we monitored cells expressing quadruple Venus-tagged Whi5 (Whi5-qV), which localizes to the nucleus when CDK1 activity is low (18). Interestingly, cells that are subjected to mechanostress progress through the cell cycle predominantly arresting with nuclear accumulation of Whi5-qV (Fig. 1*G* and Fig. S2*A* and Movie S2). However, we also observe that some cells accumulate Whi5-qV in the nucleus even after bud emergence (Fig. S2*B*, indicated by white triangle). After stress release, cell cycle efficiently restarted, as indicated by cytoplasmic relocation of Whi5-qV. Taken together, these data indicate that cells exposed to mechanostress inhibit CDK1 and slow cell cycle progression.

Calcium Signaling and Cell Wall Integrity Pathways Are Required for Cell Survival Under Mechanostress. To investigate the signaling pathways activated by mechanostress, we monitored the translocation of specific reporter proteins. Many stress signals trigger nuclear accumulation of the general stress response transcription factor Msn2 (19). Indeed, Msn2-GFP rapidly accumulated in the nucleus of cells exposed to mechanostress (Fig. 2*A*). Quantitation revealed that the response was transient, with a maximal amplitude approximately 3 min after mechanostress application (Fig. 2*A*, *Lower*). Moreover, pulses or step-wise application of compressive stress confirmed that the cellular response to mechanical stress was rapidly reversible (Fig. S3 *A* and *B*). The Msn2-GFP variant (Msn2-NLS-GFP; NLS, nuclear localization signal) specifically reporting on glucose starvation (19) did not react to mechanostress, indicating that the cellular response is

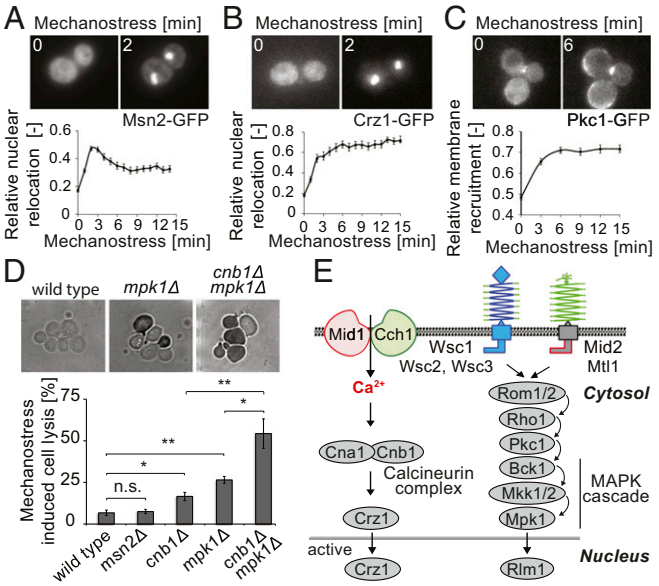

Fig. 2. Mechanostress sensitive signaling pathways in budding yeast. (*A–C*) The localization of GFP-tagged (*A*) Msn2 (Msn2-GFP), (*B*) Crz1 (Crz1-GFP), and (*C*) Pkc1 (Pkc1-GFP) was monitored at the times indicated (minutes) after applying pressure (7 psi), and the relative relocalization to the (*A* and *B*) nucleus or (*C*) plasma membrane was quantified (*Lower*). Maximum intensity projected representative images before and after 2 min of mechanostress are depicted (*Upper*). The error bars represent SEM for at least 50 cells. (*D*) Exponentially growing wild-type and the indicated mutant cells were subjected to 3 h of continuous pressure (7 psi), and dead cells were then visualized by 0.025% trypan blue staining. Representative images after trypan blue staining are shown (*Upper*). The percentage of mechanostressed induced cell lysis was determined after subtracting cell lysis in control cell chambers without pressure (*Lower*). The error bars indicate SEM from at least three experiments, each with more than 500 cells counted. A Student's *t* test was performed, and the statistical significance is indicated [not significant (n.s.) = $P > 0.05$; *$P \leq 0.05$; **$P \leq 0.01$]. (*E*) Schematic representation of the signaling pathways relevant for mechanostress transduction (21, 36). The stretch-activated calcium channel composed of Mid1 and Cch1 allows influx of calcium, thereby activating the calcineurin complex, which, in turn, triggers nuclear translocation of Crz1. The CWI pathway is activated by the putative plasma membrane sensors Mid2, Mtl1, and Wsc1-3, leading to Rho1-dependent membrane recruitment of Pkc1 and, in turn, activation of the Mpk1/Slt2 MAP kinase cascade. The stretch-sensitive extracellular domains of the postulated mechanostress sensors are indicated as springs. Images are taken with objective lens (magnification: *A–D*, 60×).

not mediated by PKA activation (Fig. S3 *C* and *D*). Nuclear translocation of the Ca^{2+}-responsive transcription factor Crz1-GFP followed similar kinetics, but, in contrast to Msn2, the response was sustained as long as the pressure was maintained (Fig. 2*B* and Movie S4). Activation of Crz1 was dependent on the presence of extracellular Ca^{2+} (Fig. S4*A*), suggesting that this response requires rapid Ca^{2+} influx. Finally, mechanostress triggered rapid and sustained activation of the CWI pathway, as visualized by the rapid translocation of Pkc1-GFP to the plasma membrane (Fig. 2*C*). Pkc1-GFP was recruited almost uniformly along the plasma membrane (Movie S5), in contrast to general cell wall stress conditions, where Pkc1 remains predominantly enriched at the bud tip or bud neck (Fig. S4*B*). Together, these results suggest that, in addition to the transient general stress response, mechanostress rapidly activates a sustained calcium response and the Pkc1/Mpk1 pathway.

To test whether these mechanostress responsive pathways are important functionally, we monitored viability of cells exposed to continued mechanostress for 3 h. While only a small portion of wild-type or *msn2Δ* cells lyse under these conditions, cells lacking the regulatory component of calcineurin, Cnb1, and the MAPK of the CWI pathway, Mpk1, greatly increased cell lysis in response to mechanostress (Fig. 2*D*). Interestingly, simultaneous deletion of *CNB1* and *MPK1* strongly exacerbated cell lysis, implying that calcium signaling and the CWI pathway have additive roles in conferring cell survival under mechanostress. Consistent with these observations, inhibition of calcineurin using FK506 in wild-type and *mpk1Δ* strains showed comparable cell lysis to *cnb1Δ* and *cnb1Δmpk1Δ* strains, respectively (Fig. S4*C*). Thus, cell survival upon mechanostress requires sustained activation of the calcineurin complex and the Pkc1/Mpk1 pathway (Fig. 2*E*). Interestingly, Mpk1 is essential to arrest cells with Whi5-qV in the nucleus, which may, in part, confer cell survival under compressive stress conditions (Fig. S4*D*).

The Calcium Channel Proteins Mid1/Cch1 and the Putative Cell Surface Protein Mid2 Sense Mechanostress and Activate Appropriate Cellular Responses. We next asked how mechanical forces are sensed and transmitted to activate calcium and CWI signaling, using translocation of Crz1-GFP and Pkc1-GFP as functional readouts. Intracellular Ca^{2+} is known to rapidly increase by a calcium channel composed of Mid1 and Cch1, while five putative cell surface proteins function upstream of the CWI pathway and could thus potentially function as mechanosensors (Fig. 2*E*). Indeed, nuclear accumulation of Crz1-GFP upon mechanostress was greatly impaired in *mid1Δ* or *cch1Δ* cells (Fig. 3 *A* and *B*). Close inspection of single-cell traces in *mid1Δ* or *cch1Δ* cells revealed heterogeneous responses, with a minor fraction of cells responding to the stress in an oscillatory manner (Fig. S4*E*). These observations suggest that mechanostress opens the Mid1-Cch1 channel, allowing influx of extracellular calcium ions, which, in turn, activate the calcineurin complex. The oscillatory dynamics of Crz1-GFP in *mid1Δ* or *cch1Δ* mutants can be attributed to additional layers of regulation, most likely from intracellular calcium sources. Surprisingly, cells lacking *MID2,* but not other cell surface receptors linked to the CWI, exhibited impaired membrane enrichment of Pkc1-GFP (Fig. 3 *C* and *D*), implying that the pressure applied by our device is specifically sensed and transduced by a single transmembrane receptor. Although TORC2 is activated by membrane stress via eisosomes and functions upstream of Pkc1 (15), we did not observe additional lysis in cells lacking structural or signaling components of eisosomes (Fig. S4*F*). Instead, the GTPase Rho1 may mediate Mid2-dependent activation of Pkc1 and Mpk1, since a GFP fusion protein reporting on Rho1 activation is rapidly recruited to the plasma membrane upon mechanostress (Fig. S4*G*). Consistent with a role as sensor of mechanical compression, Mid2-GFP localized uniformly at the plasma membrane (Fig. S5*A*), in contrast to Wsc1, which is predominantly found at sites of polarized growth (20). Interestingly, Mid2-GFP was enriched at the membrane upon exposure to mechanical force, while it accumulates at sites of polarized growth in cells treated with sodium vanadate (Fig. S5 *A–C*).

The identified mechanosensors are functionally important, as cells deleted for *MID1* and *MID2* exhibit significantly increased cell death when exposed to mechanostress (Fig. 3*E*). As expected, *mid1Δcch1Δ* cells lacking both subunits of the calcium channel did not show an additive viability defect. In contrast, *mid1Δmid2Δ* double mutants showed increased cell death compared with the single mutants, although the defect was less pronounced than that of *cnb1Δmpk1Δ* double mutants, possibly due to activation of calcineurin by intracellular calcium sources. Taken together, we conclude that the calcium channel proteins Mid1 and Cch1 together with Mid2 sense compressive stress and activate calcium signaling and the CWI pathway, respectively, to arrest cell cycle progression and prevent cell lysis.

Mid2 is a putative cell surface sensor composed of an N-terminal serine−threonine-rich (STR) domain and a C-terminal cytoplasmic tail (CT) (21). Interestingly, the STR domain has been demonstrated to behave like a linear spring in atomic force microscopy (AFM) studies (22). Although GFP-tagged Mid2

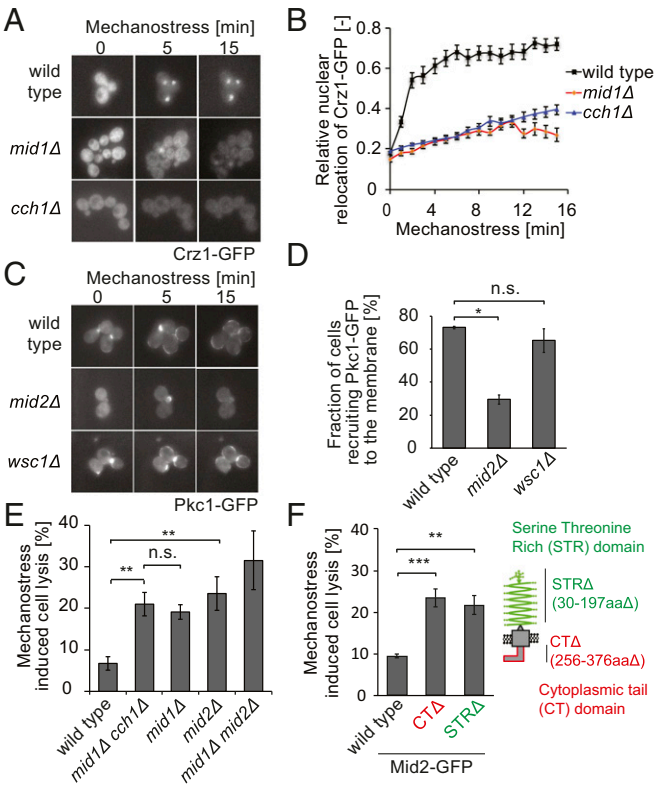

Fig. 3. Mid1/Cch1 and Mid2 function as compressive mechanosensors and activate calcium signaling and Pkc1/Mpk1 pathway, respectively. (*A*) Nuclear shuttling of Crz1–GFP upon mechanostress was analyzed by fluorescence microscopy in wild-type and the indicated mutant strains. Representative images are shown. (*B*) The relative Crz1–GFP translocation was quantified and plotted against time after applying pressure (minutes). The error bars indicate SEM for at least 50 cells analyzed for each time point and mutant. (*C*) Membrane recruitment of Pkc1-GFP in wild-type and indicated strains under mechanostress conditions. Representative images are shown. (*D*) The fraction of cells recruiting Pkc1-GFP to the membrane upon exposure to mechanostress for 15 min was determined for wild-type, *mid2Δ*, and *wsc1Δ* cells. SEM for three different experiments is indicated as error bar. (*E*) Exponentially growing wild-type and the indicated mutant strains were exposed to mechanostress for 3 h. Cell lysis was assessed by trypan blue staining and quantified after subtracting basal cell death levels in nonstressed controls. The error bars indicate the SEM for at least three experiments. (*F*) The N-terminal STR domain and the C terminus CT of Mid2 (schematically indicated in the right drawing) are functionally important for mechanostress responses. The *mid2Δ* cells expressing from its endogenous promoter Mid2-GFP, Mid2-GFP CTΔ, or Mid2-GFP STRΔ were subjected to mechanostress, and cell lysis was quantified by trypan blue staining as described in *E*. The error bars represent SEM for at least four experiments. A Student's *t* test was performed, and the significance compared with wild-type controls is indicated [not significant (n.s.) = $P > 0.05$; *$P \leq 0.05$; **$P \leq 0.01$; ***$P \leq 0.001$]. Images are taken with objective lens (magnification: *A* and *C*, 60×).

lacking the STR or CT domain were expressed to a similar level and localized to the plasma membrane like in wild-type cells, they did not rescue the cell lysis phenotype of *mid2Δ* cells exposed to mechanostress (Fig. 3*F* and Fig. S5*D*). Likewise, both domains were required for Mid2 to prevent pheromone-induced cell lysis (Fig. S5*E*), demonstrating that extracellular sensing and intracellular signaling capacities of Mid2 are functionally important to mediate efficient mechanostress responses in budding yeast.

Prevention of Polarized Cell Growth Is Crucial to Avoid Mechanostress-Induced Cell Lysis. We next investigated how the activated signaling pathways protect cells from lysis. Interestingly, we observed that about 48% of cells lyse when they possess a bud that is less than 25% of the mother cell size in *mid2Δ* cells (Fig. 2*D*, *Upper*), indicating that cells undergoing polarized growth may be more sensitive to mechanostress. Polarized growth requires polarized assembly of the actin cytoskeleton, where the formin Bni1 nucleates actin cables at growth sites to allow targeted delivery of exocytic vesicles. To investigate whether mechanostress interferes with polarized actin assembly, we synchronized the cell cycle of wild-type and *mid2Δ* cells and applied mechanostress when they formed small buds. As expected, cells not exposed to mechanical forces had polarized actin cables emanating from the bud tip and reaching into the mother cell (Fig. 4*A*). Moreover, actin patches were enriched at the bud tip, with very few patches in the mother cell. Upon application of mechanostress, wild-type cells lost most of the actin cables, and numerous actin patches redistributed to the mother cell (Fig. 4 *A* and *B*). In contrast, polarized actin structures remained largely unaffected in *mid2Δ* cells, implying that Mid2-mediated mechanosensing interferes with actin polarization, thereby preventing polarized growth. To examine whether blocking actin polarization may be functionally important, we compared cell lysis of *mid2Δ* and *mid2Δbni1Δ* cells, which are partially defective for polarized growth at bud emergence. Indeed, the cell lysis defect of *mid2Δ* was partially rescued in *mid2Δbni1Δ* double mutants (Fig. 4*C*). To corroborate these results, we also used latrunculin B (LatB), a compound that specifically disrupts

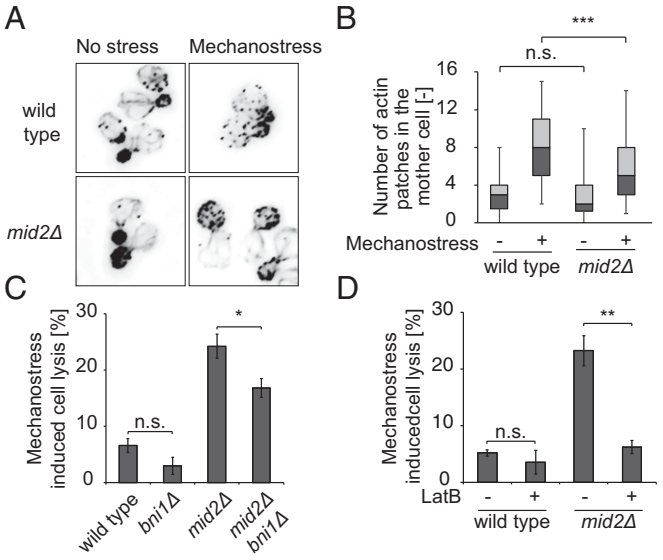

Fig. 4. Inhibition of polarized growth prevents cell lysis upon mechanostress. (*A*) Wild-type or *mid2Δ* cells were synchronized and exposed (*Right*) or not (*Left*) to mechanostress for 30 min shortly after bud emergence. Actin cables and patches were then stained with rhodamine phalloidin. Images are taken with objective lens (magnification: 100×). (*B*) The number of actin patches in the mother cell was quantified in three independent experiments with at least 50 cells using a Fiji macro script from deconvolved images. The image quantification is represented as a box–whisker plot, where 5th, 25th, 50th, 75th, and 95th percentiles are depicted. Note that mechanostress signaled by Mid2 interferes with the assembly of a polarized actin network. (*C*) Deletion of the actin nucleator Bni1 partially rescues the cell lysis defect of *mid2Δ* cells. Exponentially growing wild-type and the indicated mutant cells were exposed to mechanostress for 3 h, and the percentage of cell lysis was quantified after trypan blue staining. The experiment was performed at least three times for each strain, with over 500 cells counted for each experiment. (*D*) Actin cables of exponentially growing wild-type and *mid2Δ* cells were depolymerized by treatment with 200 μM LatB for 15 min (+), before mechanostress was applied for 3 h. Control cells were treated with the solvent DMSO (–). The percentage of cell lysis was quantified after trypan blue staining from at least three experiments with more than 500 cells counted in each case. A Student's *t* test was performed, and the significance is indicated [not significant (n.s.) = $P > 0.05$; *$P \leq 0.05$; **$P \leq 0.01$; ***$P \leq 0.001$].

actin cables. As shown in Fig. 4*D*, addition of LatB strongly reduced mechanostress induced lysis of *mid2Δ* cells. While treatment of LatB resulted in depolarized cells which are occasionally binucleated (Fig. S6*A*), deletion of *BNI1* did not cause any growth defect or affect the nuclear relocation of Msn2 and Crz1 and membrane enrichment of Pkc1 (Fig. S6 *B–E*). Moreover, while LatB treatment alone triggered nuclear relocation of Msn2, it did not interfere with mechano-induced relocation of Crz1 or Pkc1 (Fig. S6 *C–E*). Based on these results, we conclude that activation of the mechanosensor Mid2 triggers depolarization of the actin cytoskeleton, which is critical to inhibit polarized growth and thereby prevent cell lysis upon mechanostress.

Mechanostress Reverses Alpha-Factor–Induced Cell Polarization by Inhibiting Fus3 Activity in a Pkc1-Dependent Manner. To substantiate and extend these observations, we next analyzed haploid *MAT***a** cells undergoing polarized growth when exposed to **α**-factor, which results in a profound morphological shape change called shmoo. As expected, shmooing cells exhibit a polarized actin cytoskeleton with actin patches concentrated at shmoo tips, the sites of polarized growth (Fig. S7*A*). After applying mechanostress, the actin patches rapidly dispersed throughout the cell in an Mid2-dependent manner (Fig. 5*A* and Fig. S7*A*), concomitant with discontinued polarized growth (Fig. S7 *B* and *C*), and Pkc1-GFP relocalized from shmoo tips to the plasma membrane (Fig. S7*D*). Likewise, Bni1-qV dispersed from the shmoo tip and was recruited along the periphery in wild-type cells (Fig. 5 *B* and *C*), where Bni1-qV colocalized with actin patches as visualized by costaining with rhodamine phalloidin (Fig. S7*E*). In contrast, Bni1-qV remained at shmoo tips in *mid2Δ* cells and when Pkc1 activity was inhibited by the addition of cercosporamide (Fig. 5 *B–D*). Unlike Mid2, inhibition of Pkc1 activity did not hinder membrane recruitment of Bni1 as much (Fig. 5*D*), consistent with the notion that activation of the GTPase Rho1 by Rom2 may be responsible for this effect (Fig. S4*G*). Instead, Pkc1 activity was required for the dispersal of Bni1 from the shmoo tip (Fig. 5*D*). Surprisingly, Bni1-qV relocalization was unaffected in *mpk1Δ* cells, indicating that an unknown Pkc1 substrate may trigger its removal from sites of polarized growth. Taken together, these results confirm that mechanostress in shmooing cells is sensed by Mid2, which, in turn, activates Pkc1 to interfere with polarized actin assembly, at least in part by removing the actin nucleator Bni1 from shmoo tips.

Polarized growth in response to **α**-factor is driven by the MAP kinase Fus3, which is activated downstream of the pheromone receptor Ste2. Interestingly, mechanostress applied to shmooing cells results in rapid inactivation of Fus3 activity (Fig. S7*F*), as monitored by the recently described synthetic kinase activity relocation (SKAR) reporter (23). Indeed, specific inhibition of Fus3 activity by the addition of the NaPP1 inhibitor to shmooing *fus3-as1* strains triggered disassembly of the polarized growth machinery, as visualized by the prompt removal of Bni1-qV from shmoo tips (Fig. 5 *E* and *F*). These results imply that continued Fus3 activity is needed to maintain polarized growth under these conditions. On the other hand, inhibition of Pkc1 using cercosporamide stabilizes Bni1 at the shmoo tip (Fig. 5*D*). Thus, activation of Pkc1 inhibits Fus3 activity and thereby reverses pheromone-mediated cell polarization. These results uncovered an important cross-talk mechanism functionally linking the CWI and pheromone MAPK pathways, which operate during shmoo formation to rapidly block actin polarization under conditions of compressive mechanical stress.

Discussion

Here we developed and exploited a microfluidic device that elicits compressive mechanostress to single budding yeast cells. While compressive mechanical stress applied with our device activates several signaling pathways including the general stress

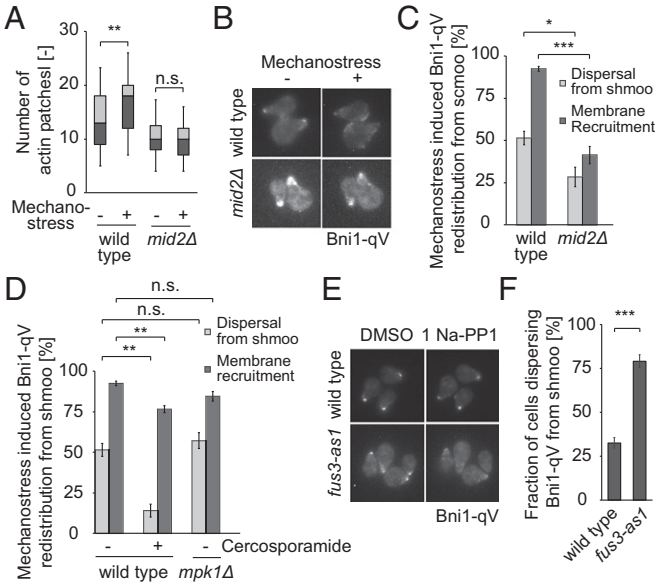

Fig. 5. Mechanostress reverses alpha-factor induced cell polarization by inhibiting Fus3 activity in a Pkc1-dependent manner. (*A*) Redistribution of the yeast actin cytoskeleton of cells polarized with alpha-factor for 90 min and exposed to mechanostress for 30 min. The actin cytoskeleton was stained with rhodamine phalloidin. The number of actin patches in the cell body exposed (+) or not (–) to mechanostress was quantified after deconvolution, and shown as box–whisker plots, which depict 5th, 25th, 50th, 75th, and 95th percentiles of actin foci. At least 50 cells were analyzed for each experiment. (*B*) Redistribution of Bni1 away from shmoo tips after mechanostress. Wild-type or *mid2Δ* cells expressing Bni1-qV were exposed to alpha-factor for 90 min, and the polarized cells were subjected to mechanostress. Maximum intensity projected images of cells prior to (–) and after 15 min of mechanostress (+) are shown. (*C*) Quantification of images from *B*. The dynamics of Bni1-qV under mechanostress was quantified in terms of dispersal from the shmoo tip and recruitment to the plasma membrane away from the shmoo tip. The percentage of cells that dispersed or recruited Bni1 is depicted in the graph. The experiment was performed three times with at least 50 cells counted for each condition. (*D*) Dynamics of Bni1-qV with mechanostress at the indicated conditions was quantified as in *C*. (*E*) Analog-sensitive *fus3-as1* cells expressing Bni1-qV were polarized with alpha-factor for 90 min, and Bni1-qV redistribution was monitored after inhibiting Fus3 activity with 1Na-PP1 for 20 min. (*F*) Quantification of Bni1 dispersal away from shmoo tips upon mechanostress. The fraction of cells that dispersed more than 25% of Bni1, quantified by measuring the Bni1 intensity at the 4 pixel × 4 pixel brightest area is represented for each condition. The experiment was performed three times, and at least 50 cells were counted for each condition. A Student's *t* test was performed and the statistical significance is indicated [not significant (n.s.) = $P > 0.05$; *$P \leq 0.05$; **$P \leq 0.01$; ***$P \leq 0.001$]. Images are taken with objective lens (magnification: *B* and *E*, 60×).

response, calcium signaling and the Pkc1/Mpk1 pathway cooperate functionally to protect cells from lysis by preventing cell cycle progression and polarized growth. The isotropic localization of Pkc1 around the cell membrane may ensure cell survival under compressive stress by redirecting cell wall biosynthesis. Moreover, activation of Mpk1 leads to Sic1 stabilization, thereby inhibiting the G1/S transition (24). However, the role of the Ca^{2+}/calcineurin pathway is less clear. Calcineurin may contribute to cell survival by promoting transcription of cell wall synthesis genes such as *FKS2* (25), or regulate cytoskeletal dynamics and intracellular trafficking (26, 27), processes that contribute to polarized growth. In addition, the Ca^{2+}/calcineurin pathway may converge on Pkc1 activity, possibly by increasing $PI_{4,5}P_2$ in the plasma membrane via synaptojanins (28, 29).

Our results demonstrate that Mid1/Cch1 and Mid2 specifically sense compressive stress in the plasma membrane, and activate intracellular Ca^{2+}/calcineurin and Pkc1/Mpk1 pathways, respectively.

CELL BIOLOGY

While Mid1 in complex with Cch1 forms a stretch-activated Ca^{2+} channel (30, 31), the cytoplasmic domain of Mid2 binds and activates Rom2/Rho1 upon mechanostress (21). Mid2 possesses STR extracellular domains, which confer nanospring-like mechanical properties (22). Interestingly, both domains are required for the mechanostress function of Mid2 in vivo, implying stress sensing and intracellular signal transduction activity, respectively. Other members of the Wsc family also contain STR domains, and we speculate that they are dedicated to sense specific types of mechanical forces. It will thus be interesting to investigate how the apparently similar STR domains are able to spatially and temporally respond to different insults, including shear stress and stretching.

Calcium signaling and MAP kinase signaling pathways are also activated in response to mechanical stimuli in mammals. For instance, Erk5 ensures survival of endothelial cells exposed to shear stress, and its activation triggers epithelial-to-mesenchymal transition (EMT) (32). Likewise, mechanical stress leads to Ca^{2+} influx resulting in calcineurin/NFAT activation, which is essential for mammary tumorigenesis and metastasis (33). Unlike the yeast Mid1/Cch1, the mammalian Ca^{2+} channel protein polycystin1/polycystin2 possesses an extracellular Wsc domain, described first for yeast, which may sense the mechanical signal. Although compressive stress up to about 2 psi to 3 psi (15 kPa to 20 kPa) was measured in the microenvironment of solid tumors (34, 35), how such physical stimuli lead to EMT remains to be established. A recent study revealed that the Bni1 homolog FMN2 is redistributed and recruits perinuclear actin during migration of cells through narrow constrictions (12). Moreover, depolarized cells become more flexible and less susceptible to high pressure and shear stress as they travel to ectopic sites. Thus, similar to budding yeast, cytoskeletal reorganization and altered cell polarity may ensure cell survival under mechanical compression. Understanding how mechanical stress alters cell polarity and leads to metastasis may provide promising strategies of therapeutic intervention for cancer and other diseases that have deregulated mechano-sensitive feedback mechanisms such as muscular dystrophy, cardiomyopathies, and polycystic kidney disease.

Materials and Methods

All plasmids and yeast strains are listed in Tables S1 and S2, respectively. The microfluidic device was constructed by soft lithography and mounted on the stage of the microscope for live-cell imaging. Detailed information of *materials and methods* is provided in *Supporting Information*.

ACKNOWLEDGMENTS. We thank S. Pelet for the SKAR reporter, D. Pellman for sharing the Rho1 biosensor, and J. Tilma for help with strain construction. We are grateful to A. Smith and S. Jha for critical reading of the manuscript, and J. Thorner, R. Loewith, and members of the M.P. laboratory for helpful discussions. Work in the M.P. laboratory is funded by the ETH Zürich, the European Research Council (ERC), SystemsX.ch, the Swiss National Foundation (SNF), and the Global Research Laboratory (Grant NRF-2015K1A1A2033054) of the Korean National Research Foundation (NRF). The N.L.J. laboratory is supported by the Basic Science Research Program funded by the Korean Ministry of Science and the ICT & Future Planning (Grant NRF-2015R1A2A1A09005662). Both the N.L.J. and the M.P. laboratories were supported by the Strategic Korean–Swiss Cooperative Program (2009-00525).

1. Wirtz D, Konstantopoulos K, Searson PC (2011) The physics of cancer: The role of physical interactions and mechanical forces in metastasis. *Nat Rev Cancer* 11:512–522.
2. Fukuda S, Yasu T, Predescu DN, Schmid-Schönbein GW (2000) Mechanisms for regulation of fluid shear stress response in circulating leukocytes. *Circ Res* 86:E13–E18.
3. Moazzam F, DeLano FA, Zweifach BW, Schmid-Schönbein GW (1997) The leukocyte response to fluid stress. *Proc Natl Acad Sci USA* 94:5338–5343.
4. Su SS, Schmid-Schönbein GW (2008) Fluid stresses on the membrane of migrating leukocytes. *Ann Biomed Eng* 36:298–307.
5. Shirai A, Masuda S (2013) Numerical simulation of passage of a neutrophil through a rectangular channel with a moderate constriction. *PLoS One* 8:e59416.
6. Jain RK, Martin JD, Stylianopoulos T (2014) The role of mechanical forces in tumor growth and therapy. *Annu Rev Biomed Eng* 16:321–346.
7. Tse JM, et al. (2012) Mechanical compression drives cancer cells toward invasive phenotype. *Proc Natl Acad Sci USA* 109:911–916.
8. Liu YJ, et al. (2015) Confinement and low adhesion induce fast amoeboid migration of slow mesenchymal cells. *Cell* 160:659–672.
9. Macek Jilkova Z, et al. (2014) CCM proteins control endothelial β1 integrin dependent response to shear stress. *Biol Open* 3:1228–1235.
10. Matthews BD, Overby DR, Mannix R, Ingber DE (2006) Cellular adaptation to mechanical stress: Role of integrins, Rho, cytoskeletal tension and mechanosensitive ion channels. *J Cell Sci* 119:508–518.
11. Tzima E, del Pozo MA, Shattil SJ, Chien S, Schwartz MA (2001) Activation of integrins in endothelial cells by fluid shear stress mediates Rho-dependent cytoskeletal alignment. *EMBO J* 20:4639–4647.
12. Skau CT, et al. (2016) FMN2 makes perinuclear actin to protect nuclei during confined migration and promote metastasis. *Cell* 167:1571–1585.
13. AbouAlaiwi WA, et al. (2009) Ciliary polycystin-2 is a mechanosensitive calcium channel involved in nitric oxide signaling cascades. *Circ Res* 104:860–869.
14. Nauli SM, et al. (2003) Polycystins 1 and 2 mediate mechanosensation in the primary cilium of kidney cells. *Nat Genet* 33:129–137.
15. Berchtold D, et al. (2012) Plasma membrane stress induces relocalization of Slm proteins and activation of TORC2 to promote sphingolipid synthesis. *Nat Cell Biol* 14: 542–547.
16. Delarue M, et al. (2016) Self-driven jamming in growing microbial populations. *Nat Phys* 12:762–766.
17. Delarue M, et al. (2017) SCWISh network is essential for survival under mechanical pressure. *Proc Natl Acad Sci USA* 114:13465–13470.
18. Costanzo M, et al. (2004) CDK activity antagonizes Whi5, an inhibitor of G1/S transcription in yeast. *Cell* 117:899–913.
19. Görner W, et al. (2002) Acute glucose starvation activates the nuclear localization signal of a stress-specific yeast transcription factor. *EMBO J* 21:135–144.
20. Piao HL, Machado IMP, Payne GS (2007) NPFXD-mediated endocytosis and function of a yeast cell is required for polarity wall stress sensor. *Mol Biol Cell* 18:57–65.
21. Levin DE (2011) Regulation of cell wall biogenesis in *Saccharomyces cerevisiae*: The cell wall integrity signaling pathway. *Genetics* 189:1145–1175.
22. Dupres V, et al. (2009) The yeast Wsc1 cell surface sensor behaves like a nanospring in vivo. *Nat Chem Biol* 5:857–862.
23. Durandau E, Aymoz D, Pelet S (2015) Dynamic single cell measurements of kinase activity by synthetic kinase activity relocation sensors. *BMC Biol* 13:55.
24. Moreno-Torres M, Jaquenoud M, De Virgilio C (2015) TORC1 controls G1-S cell cycle transition in yeast via Mpk1 and the greatwall kinase pathway. *Nat Commun* 6:8256.
25. Stathopoulos AM, Cyert MS (1997) Calcineurin acts through the CRZ1/TCN1-encoded transcription factor to regulate gene expression in yeast. *Genes Dev* 11:3432–3444.
26. Bultynck G, et al. (2006) Slm1 and slm2 are novel substrates of the calcineurin phosphatase required for heat stress-induced endocytosis of the yeast uracil permease. *Mol Cell Biol* 26:4729–4745.
27. Fadri M, Daquinag A, Wang S, Xue T, Kunz J (2005) The pleckstrin homology domain proteins Slm1 and Slm2 are required for actin cytoskeleton organization in yeast and bind phosphatidylinositol-4,5-bisphosphate and TORC2. *Mol Biol Cell* 16:1883–1900.
28. Goldman A, et al. (2014) The calcineurin signaling network evolves via conserved kinase-phosphatase modules that transcend substrate identity. *Mol Cell* 55:422–435.
29. Guiney EL, Goldman AR, Elias JE, Cyert MS (2015) Calcineurin regulates the yeast synaptojanin Inp53/Sjl3 during membrane stress. *Mol Biol Cell* 26:769–785.
30. Fischer M, et al. (1997) The Saccharomyces cerevisiae CCH1 gene is involved in calcium influx and mating. *FEBS Lett* 419:259–262.
31. Peiter E, Fischer M, Sidaway K, Roberts SK, Sanders D (2005) The *Saccharomyces cerevisiae* Ca2+ channel Cch1pMid1p is essential for tolerance to cold stress and iron toxicity. *FEBS Lett* 579:5697–5703.
32. Drew BA, Burow ME, Beckman BS (2012) MEK5/ERK5 pathway: The first fifteen years. *Biochim Biophys Acta* 1825:37–48.
33. Quang CT, et al. (2015) The calcineurin/NFAT pathway is activated in diagnostic breast cancer cases and is essential to survival and metastasis of mammary cancer cells. *Cell Death Dis* 6:e1658.
34. Stylianopoulos T, et al. (2013) Coevolution of solid stress and interstitial fluid pressure in tumors during progression: Implications for vascular collapse. *Cancer Res* 73: 3833–3841.
35. Stylianopoulos T, et al. (2012) Causes, consequences, and remedies for growth-induced solid stress in murine and human tumors. *Proc Natl Acad Sci USA* 109: 15101–15108.
36. Chow EW, et al. (2017) Elucidation of the calcineurin-Crz1 stress response transcriptional network in the human fungal pathogen Cryptococcus neoformans. *PLoS Genet* 13:e1006667.